Adaptive hybrid optimal quantum control for imprecisely characterized systems

D. J. Egger and F. K. Wilhelm
Theoretical Physics, Universität des Saarlandes, D-66123 Saarbrücken, Germany

Optimal quantum control theory carries a huge promise for quantum technology. Its experimental application, however, is often hindered by imprecise knowledge of the its input variables, the quantum system's parameters. We show how to overcome this by Adaptive Hybrid Optimal Control (Ad-HOC). This protocol combines open- and closed-loop optimal by first performing a gradient search towards a near-optimal control pulse and then an experimental fidelity measure with a gradient-free method. For typical settings in solid-state quantum information processing, Ad-Hoc enhances gate fidelities by an order of magnitude hence making optimal control theory applicable and useful.

PACS numbers: 02.30.Yy, 03.67.-a, 67.85.-d

arXiv:1402.7193v1 [quant-ph] 28 Feb 2014

The last decades have seen the transformation of quantum theory from a mere description of nature to a tool in research and applications, prominently in quantum information processing [1], spectroscopy, sensing, and metrology [2]. Quantum control describes the science of shaping the time evolution of quantum systems in a potentially useful way [3, 4]. Control parameters typically are parameters of an external field parameterized in a technologically appropriate way, e.g., into a quantum logic gate [5], into a higher coherence in NMR [6–8], or into states important for sensing[9]. While analytically accessible only in highly specialized cases, these pulse shapes can in many cases be found using the powerful mathematical technique of Optimal Control Theory (OCT); by solving a Schrödinger or master equation iteratively, a pulse shape producing the desired time evolution can be found [6]. This results in complex pulses that are used in a wide variety of cases such as controlling the cooperative effects of driving and dissipation [10], to control non-integrable quantum many-body [11] and many electron [12] systems, generating matter-wave entanglement [13, 14] and quantum information devices [15–17]. These pulses are designed based on the best available knowledge of the system. This can be insufficient for two reasons i) In many cases, the underlying model cannot be solved with sufficient precision as in the case of many-body systems [12] ii) in quantum systems that are engineered or when a human-made apparatus is a key part of the setup, parameters need to be measured with precision compatible with the control task at hand [18], which is often not possible. This necessity to precisely know the underlying model strongly limits harvesting the benefits of optimal control in complex quantum systems.

In this Letter we solve this problem with a hybrid open/closed-loop optimal control method called Adaptation by hybrid optimal control (Ad-HOC). It is designed to overcome shortcomings of the assumed physical model [19], errors on the controls themselves and inaccurate knowledge of the parameters. It starts with a gradient search on a model with the best reasonably achievable accuracy. Ad-HOC then uses the physical system itself as a feed-back to calibrate the control pulses. The gradient search approaches a favorable control over a large distance based on theory and simulation whilst the closed-loop design, done directly on the experiment, takes into account all experimental details [20]. Additionally, the performance index in gradient search can impose additional conditions such as limitations to the fields or robustness. We demonstrate this approach along two tasks: We first show that pulses can be optimized using only feedback from the experiment. We then demonstrate the efficiency of the hybrid method for the example of two superconducting qubits[21]. The latter are particularly sensitive to calibration errors [18] making them ideal for testing Ad-HOC.

Problem setting: Delicate engineering of controlled quantum systems, in particular the need to isolate quantum systems from their environemtsn, makes quantum control setups very complex. Such an experiment, sketched in Fig. 1 is made of the system to be controlled and the unit (the AWG) producing the control pulses. The pulses are brought from the latter to the former by a chain of electronic or optical components referred to as *control transfer chain*. In this setup, four different mechanisms will degrade the fidelity of an OCT designed pulse. i) Parameter measurement: The quantum system to be controlled is modeled by a drift and control Hamiltonians $\hat{H} = \hat{H}_\mathrm{d} + \sum_i u_i(t)\hat{H}_{\mathrm{c},i}$ with $\boldsymbol{u}(t)$ the control fields to be shaped. Imprecise characterization of parameters entering the drift $\hat{H}_\mathrm{d}$ and controls $\hat{H}_{\mathrm{c},i}$ will degrade fidelity. ii) Improper characterization of the control transfer chain's distortion of the pulses [14, 22]. iii) Signal calibration: in practice the control unit generates an electrical signal or laser impulse which is related to $\boldsymbol{u}(t)$. Imprecisions in this relation, e.g. a constant offset, generate errors on the controls themselves which are notoriously hard to correct. iv) Effects that are not taken into account in $\hat{H}$. Among many examples are other idling components of a complex quantum system such as a quantum processor, spurious two level fluctuators in Josephson Junctions, as well as slow non-Markovian noise. Errors in parameters can be addressed

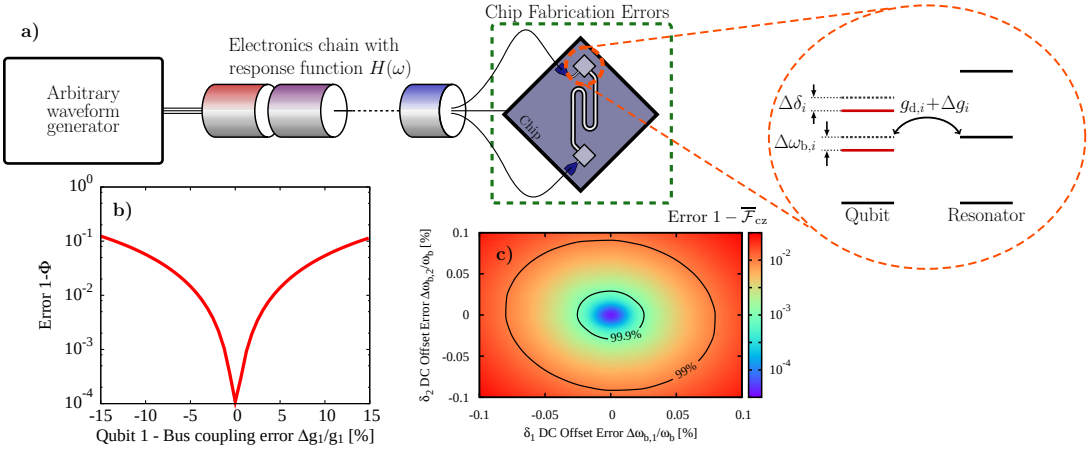

FIG. 1. (color online). a) Sketch of quantum control experiment. The unit generating the control pulses, typically an arbitrary waveform generator (AWG), at room temperature generates the control pulses that are sent through the control transfer chain (sketched as the chain of cylinders) to finally reach the quantum system, often cooled to less than a Kelvin. Error sources are in the parameters modeling the "chip", the electronics and the calibration of the control signals. Figures b) and c) relate to a CZ gate within the framework of two qubits coupled through a bus resonator. b) Degradation of a 99.99% fidelity CZ gate assuming only an error on the coupling between qubit 1 and the bus. As can be seen the gate fidelity degrades quickly. c) Degradation of CZ gate, optimized to machine precision, due to calibration errors in the qubit controls causing the resonance point with the bus to be missed by an amount $\Delta\omega_{b,i}$. The two circles indicate the 99% and 99.9% fidelity limits. Such errors heavily degrade the gate performance.

using broadband control [23, 24] which often leads to cumbersome pulses. Furthermore, no such approach is known for uncertain transfer functions. Practically, these functions as well as the linearity of the signal transfer are extremely hard to verify with the needed precision.

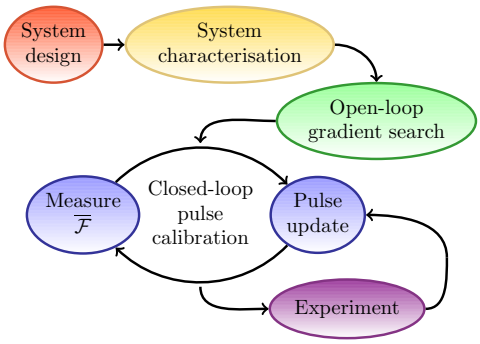

FIG. 2. (color online) Sketch of the Ad-HOC protocol. The physical system and surrounding control and measurement apparatus are designed taking control problems into consideration. The system is then characterized with the best possible precision. Using the parameters from this characterization the control pulses are created. These are then fine tuned to the system using closed-loop OCT. The pulses are then ready to be used in the experiment and can be recalibrated at a later time to account for drift.

Proposed method: In order to addres imperfections of the model, the control loop can be closed by using the experiment itself as feed-back to calibrate the control pulses. An initial gradient search [6, 25] of the optimal pulse is performed with the best model of the system. This gives control pulses that yield high fidelity on the model but perform sub-optimally in the real system. They still lie close to the optimal point in the control landscape of the actual system given that it is approximated by the model, typically in the basin of attraction of the desired minimum. A set of similar pulses (with model parameters drawn from the error bars of the initial characterization of the system) are sent to the experiment and their performance measured. The pulses are then updated and the procedure is iterated until either a target performance is reached or convergence halts. Given that it is time consuming to measure the performance of pulses we chose the Nelder-Mead algorithm [26]. It is robust and typically only evaluates 1-2 pulses per iteration. Once the calibration is done, the pulses can be used. At a latter time a few pulse calibration iterations correct for drifts in parameter values and experiments can resume. The Ad-HOC protocol is illustrated in Fig. 2. Note that the precise experimental parameters are never identified. Also, this procedure hinges on an efficient method to experimentally measure the performance index. Here, the performance index is the process fidelity which can be measured using Randomized Benchmarking (RB) [27–29]. Other than more standard process tomography, it is significantly faster to measure and minimizes the impact of state preparation and measurement errors. RB yields the average fidelity

$$\overline{\mathcal{F}} = \int \mathrm{d}\hat{U}\, \langle\psi|\hat{U}^\dagger\hat{U}_\mathrm{t}^\dagger\Lambda(\hat{U}\,|\psi\rangle\langle\psi|\,\hat{U}^\dagger)\hat{U}_\mathrm{t}\hat{U}|\psi\rangle\,, \qquad (1)$$

measuring how well the channel Λ implements the target unitary time evolution $\hat{U}_\mathrm{t}$. As shown in [30], random-

ized benchmarking is well-adapted to fast experimentation and catches a variety of practical errors of different scales.

Closed loop demonstration: To show that a pulse can be optimized based only on its performance index we consider random gate synthesis. Inside a black box is a two level system in which the drift and control Hamiltonians are both random Hermitian matrices. The black box input is a pulse and the output its fidelity. The target is a random unitary matrix. Figure 3 shows the mean and median error as function of iteration for 100 different realizations of the two level system (see supplementary material for details). It is important to recognize in Fig. 3 that while demonstrating the power of the closed-loop part of Ad-HOC it also highlights that closed loop contol alone needs a large number of steps necessary for a rather elementary control task. Going down this convergence curve with gradient search drastically reduces the number of steps to about 50 iterations per order of magnitude error reduction.

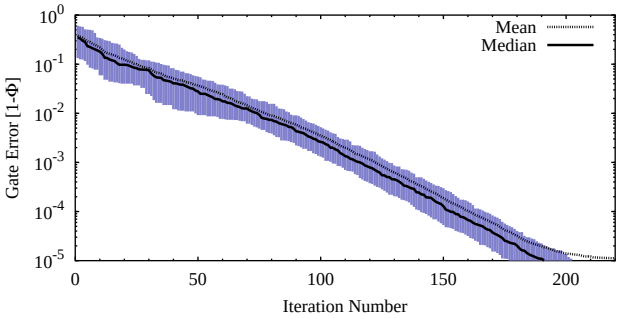

FIG. 3. (color online). Convergence plot showing the optimization of random gates. 100 pulses were optimized each for a different realization of the random two level system. The target fidelity of $1-10^{-5}$ is reached rapidly in most cases as indicated by the median. The shaded area includes 68% of all runs centered around the median.

Numerical demonstration for a realistic setting: To demonstrate hybrid optimal control in a more complicated yet realistic and genuine system, we choose to create a CZ gate between two superconducting qubits in the qubit-bus-qubit system [31]. In quantum information it is paramount to have extremely high fidelity gates [32] and the systems are well described by the typical setup of Fig. 1 with the addition that the quantum system is at the coldest stage in a dilution cryostat. The qubit-bus-qubit Hamiltonian is modeled by [33]

$$\hat{H} = \sum_i \delta_i(t)\hat{\sigma}_i^+\hat{\sigma}_i^- + \Delta_i\,|2\rangle_{i\,i}\langle 2| + \frac{g_i}{2}\left(\hat{\sigma}_i^+\hat{a} + \hat{\sigma}_i^-\hat{a}^\dagger\right) .$$

The control $\delta_i(t)$ is the i^{th} qubit-bus detuning. Δ_i the non-linearity of the qubits and g_i the coupling between each qubit and the bus. $\hat{\sigma}_i^+$ and $\hat{a}^\dagger$ respectively create an excitation in qubit i and the bus. This system is

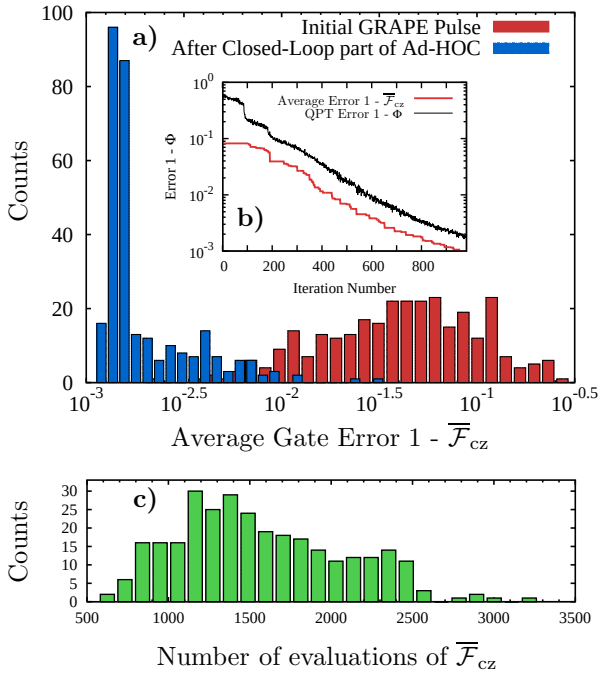

FIG. 4. (color online). Debugging procedure for parameter errors, control transfer chain errors and control DC offset errors. The error of the initial pulse was minimized using a gradient search down to machine precision. The pulses are then calibrated to a specific realization of the system. a) Histograms for 300 system realizations. The red histograms show the fidelity of the initial uncalibrated numerical pulse. The blue histograms show the improvement in average gate fidelity after running Ad-HOC. b) Gate errors as function of the calibration algorithms iteration number. c) Histograms of the number of times the average gate fidelity had to be evaluated in order to calibrate the pulse to the different system realizations, i.e. to take the red histograms to the blue ones.

particularly vulnerable to errors on the controls and parameters [18]. For instance Fig. 1b shows the degradation of fidelity due to an error on a single parameter. Fig. 1c shows the impact of a DC offset $\Delta\omega_{\text{b},i}$ on the controls caused by a miscalibration between the AWG's output voltage and the corresponding qubit frequency. This makes the qubit miss the resonance point with the bus. These examples illustrate how severely single errors can impact gate fidelities. In fact, albeit the initial numerical optimization leading to a pulse that is first-order insensitive to errors, the second derivative is large, making this an example that is specifically unforgiving to model uncertainty and the ideal case for showing Ad-HOC's performance.

First, a gradient search optimizes down to machine precision the error of a CZ gate using the quantum process fidelity $\Phi = |\text{Tr}\{\hat{U}_{\text{cz}}^\dagger \hat{U}[\delta_1,\delta_2]\}|^2/d^2$. Φ measures the overlap between the ideal CZ gate $\hat{U}_{\text{cz}}$ and the gate implemented by the controls δ_i. d is the dimension of the Hilbert space. Next, the parameters in the model g_i and Δ_i, as well as the DC offsets $\Delta\omega_{\text{b},i}$ and the standard de-

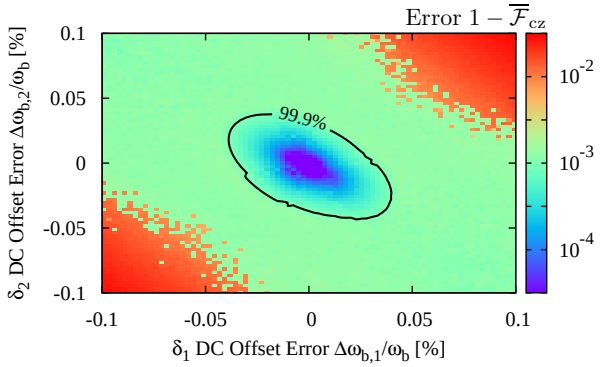

FIG. 5. (color online). Average error for the CZ gate as function of the DC offset error $\Delta\omega_{b,i}$ introduced by miscalibrating the AWG's output to the qubit frequency. Ad-HOC greatly improves the fidelity of the pulse as can be seen by comparing to Fig. 1c where the pulses found by OCT were not calibrated to the system. The central region of high fidelity does not change since the target fidelity for the calibration protocol was 99.9%.

viation of the transfer chain's impulse response are promoted to random variables following Gaussian statistics with variances reflecting the precision of actual measurements [34]. We then compute the average gate fidelity $\overline{\mathcal{F}}$ for many different realizations of the system. This is shown in Fig. 4a by the red histograms. As expected the fidelities are nowhere close to optimal ranging between 99% and 68%, clearly insufficient for quantum computing. Finally each instance is reoptimized using the closed loop part of Ad-HOC resulting in the blue histograms in Fig. 4a. Ad-HOC increased the fidelity by more than an order of magnitude. Fig. 4b shows a typical decrease in error during the closed loop optimization. As $\overline{\mathcal{F}}$ is being maximized, Φ, computed for comparison, also increases. The corresponding number of required evaluations of $\overline{\mathcal{F}}$ for each realization is shown in Fig. 4c. A further illustration of the protocol's performance is shown in Fig. 5. In this case only the control DC offset error $\Delta\omega_{b,i}$ was present. As can be seen by comparing to Fig. 1c the fidelity has been increased over a wide range of possible $\Delta\omega_{b,i}$'s. This shows how successful Ad-HOC is in dealing with errors on the controls themselves.

Robustness: In the previous examples the sampling of the integral in Eq. (1) introduces noise into the fidelity measure. Noise would also be present in an experiment but for different reasons. Here is further investigated the effect of noise on convergence. We consider the fidelity Φ which can be computed without introducing noise. A noiseless run of closed-loop optimization is compared to a noisy run. Noise is artificially added to Φ by a depolarizing channel [1] acting n times out of m with uniform probability p. The smaller m is, the more sampling noise is added to Φ. The noisy and noiseless optimizations are shown in Fig. 6, they converge at the same speed until the noisy case halts. This termination results from the increase in fidelity, averaged over several iterations, being smaller than the noise threshold $\Delta\Phi_{th.}$ (see supplementary material). The calibration protocol can no longer determine if the changes made to the pulses improve Φ and halts. This is illustrated in Fig. 6b showing the difference between successive iterations of fidelity of the worst pulse $\Phi_{w.}$ in the pulse simplex.

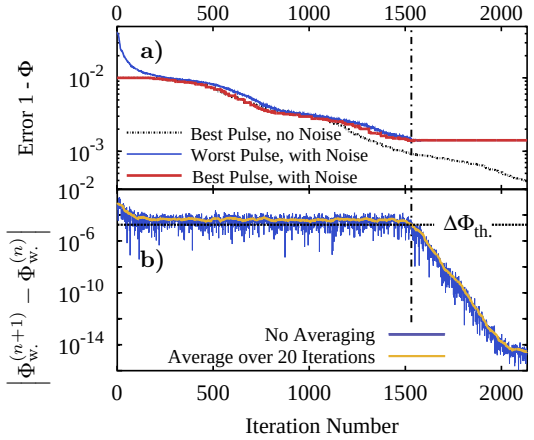

FIG. 6. (color online). a) Convergence speed of a single optimization comparing the cases when a depolarizing channel adds noise and when the optimization is noiseless. b) Difference in fidelity of the worst point in the simplex between subsequent iterations in a noisy optimization. As long as, on average, this difference is greater than the noise level, the optimization continues.

Model-free calibration was pioneered in [20] using genetic algorithms, which we typically found 1.5 orders of magnitude slower in convergence. The Nelder-Mead algorithm has been used in tuning dynamical decoupling sequences in [35] and is part of the CRAB optimal control scheme [11] without initial gradient search. The closed-loop part of Ad-HOC has been experimentally implemented for a CZ gate done between two coupled superconducting qubits [30] and enabled the high gate fidelities in [36].

In conclusion we have demonstrated Adaptive Hybrid Optimal Control (Ad-HOC), a protocol for overcoming model imperfection and incompleteness afflicting the design of control pulses for quantum systems. The protocol is efficient and can be applied to almost arbitrary quantum control experiments as it can be used with any fidelity measure that captures the essence of the desired time evolution. We showed that noise does not affect convergence speed but rather the terminal fidelity. Therefore higher fidelity can be gained by increasing the measurement precision. Ad-HOC, overcomes model inaccuracies and errors on the controls themselves.

We thank J.M. Martinis for insisting that optimal control will not be applied without calibration, M. Biercuk for pointing us to the Nelder-Mead algorithm and J. Kelly and R. Barends for pointing out the speediness of Ran-

domized Benchmarking. This work was supported by the EU through SCALEQIT and QUAINT as well as funded by the Office of the Director of National Intelligence (ODNI), Intelligence Advanced Research Projects Activity (IARPA), through the Army Research Office. All statements of fact, opinion or conclusions contained herein are those of the authors and should not be construed as representing the official views or policies of IARPA, the ODNI, or the U.S. Government.

SUPPLEMENTARY MATERIAL

In this supplementary material we give some details on the optimization of control pulses for random two level systems. We also show that a few parameter pulse can be calibrated extremely quickly. A few extra details on the qubit-bus-qubit system are given. Finally we show that the calibration does not have to be constrained to the use of randomized benchmarking. To do this we calibrate a CZ pulse using a fidelity measure tailored to the CZ gate.

Modelling of the Control Transfer Chain

The transfer chain between the quantum system and the arbitrary waveform generator (AWG) can be taken into account in the optimization [14, 22]. The difficulty is to know its effects (even nonlinearities may play a role) to high enough accuracy so as not to degrade OCT designed pulses. This in practice cannot be achieved. Here we describe how control transfer chains can be modeled and how output signals from the AWG relate to the control fields $\boldsymbol{u}(t)$ used in the Hamiltonian. The voltages $\boldsymbol{V}(t)$ produced by the AWG are not identical to the functions $\boldsymbol{u}(t)$. Instead they are related through a calibration curve $\boldsymbol{C}$. Furthermore the impulse response of the transfer chain h between the AWG and the experiment can distort the pulses. Thus whilst the AWG produces $\boldsymbol{V}(t)$ the quantum system actually receives

$$\boldsymbol{u}(t) = \int_0^t \mathrm{d}\tau \, (\boldsymbol{C} \circ \boldsymbol{V})(t-\tau)\, h(\tau). \tag{2}$$

This can be taken into account using the methodology of Ref. [22] if $\boldsymbol{C}$ and h are precisely known. Practically, these functions as well as the linearity of the signal transfer stipulated in Eq. (2) are extremely hard to verify with the needed precision. Whereas errors in parameters of the system can be addressed using broadband control [23, 24, 37], no such approach is known for uncertain transfer functions.

Control of Random Two Level Systems

To investigate the performance of the model free calibration we apply it to the control of random two level systems. The Hamiltonians are

$$\hat{H}(t) = \begin{pmatrix} H_1^{(\mathrm{d})} & H_2^{(\mathrm{d})} + iH_3^{(\mathrm{d})} \\ H_2^{(\mathrm{d})} - iH_3^{(\mathrm{d})} & H_4^{(\mathrm{d})} \end{pmatrix} + u(t) \begin{pmatrix} H_1^{(\mathrm{c})} & H_2^{(\mathrm{c})} + iH_3^{(\mathrm{c})} \\ H_2^{(\mathrm{c})} - iH_3^{(\mathrm{c})} & H_4^{(\mathrm{c})} \end{pmatrix}. \tag{3}$$

The random variable $H_i^{(\mathrm{x})} \in \mathbb{R}$ are uniformly distributed in $[-0.5, 0.5]$. For each realization of the drift $\hat{H}^{(\mathrm{d})}$ and control $\hat{H}^{(\mathrm{c})}$ a target unitary matrix $\hat{U}_{\mathrm{rand}}$, chosen randomly is given. For each realization we seek a different control $u(t)$ to optimize the fidelity $\Phi = |\mathrm{Tr}\{\hat{U}_{\mathrm{rand}}^{\dagger}\hat{U}\}|^2/4$. A histogram of the number of runs required to reach $1 - 10^{-5}$ fidelity is shown in Fig. 7. The median and mean fidelity as function of number of iterations is shown in the main text. Instances that converged poorly can be attributed to realizations that are hard to control in the given time, as the commutoator between $\hat{H}^{\mathrm{d}}$ and $\hat{H}^{\mathrm{c}}$ turns out to be too small. To confirm this statement we plot the number of times Φ was evaluated as function of the smallest relevant matrix norm, defined as

$$\eta = \max \left\{ \left\| \left[\hat{H}^{(\mathrm{d})}, \hat{H}^{(\mathrm{c})}\right] \right\|, \left\| \left[\hat{H}^{(\mathrm{d})}, [\hat{H}^{(\mathrm{d})}, \hat{H}^{(\mathrm{c})}]\right] \right\|, \left\| \left[\hat{H}^{(\mathrm{c})}, [\hat{H}^{(\mathrm{d})}, \hat{H}^{(\mathrm{c})}]\right] \right\} . \tag{4}$$

$\|\cdot\|$ is the max norm. The smaller η is, the harder the system is to control. This is reflected in Fig. 7. Overall for controllable systems the number of evaluations of Φ is low especially since the starting point for the optimization was the null control $u(t) = 0 \ \forall \ t$. At very small values of η the system tends to be uncontrollable and some target gates cannot be reached. Two bad instances were removed from the data. These had very small commutator norms and failed to converge.

Few Parameter Pulse Closed-Loop Optimization Example: Finding DRAG

In a two level system an $\hat{X}$ gate can be implemented by applying a pulse of area π on the Ω_x component of the driving field. However, when a third level is present this is no longer sufficient and DRAG pulses are needed [17, 38]. Generally, full characterization of the third level - its anharmonicity and coupling ratio, is an extra characterization step that can be avoided using Ad-HOC. The Hamiltonian for an anharmonic three level system, driven on resonance and in the frame rotating at the frequency

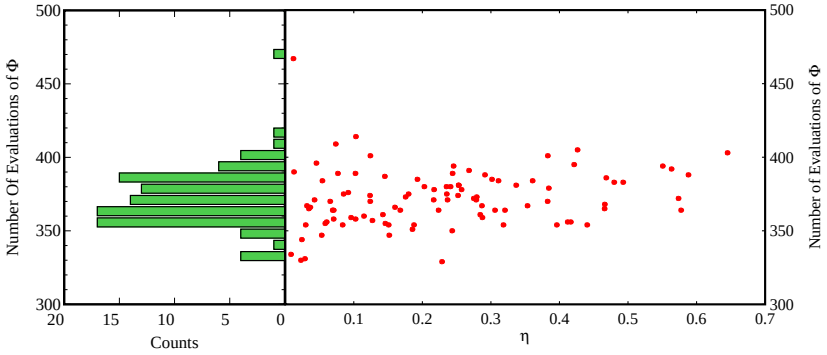

FIG. 7. (color online) Number of evaluations of the fidelity as function of the biggest relevant norm η defined in Eq. (4). In this data two points with particularly small η failed to converge and were excluded from the data.

of the drive field is

$$\hat{H} = \begin{pmatrix} 0 & 0 & 0 \\ 0 & 0 & 0 \\ 0 & 0 & \Delta \end{pmatrix} + \frac{\Omega_x(t)}{2} \begin{pmatrix} 0 & 1 & 0 \\ 1 & 0 & \sqrt{2} \\ 0 & \sqrt{2} & 0 \end{pmatrix} + i\frac{\Omega_y(t)}{2} \begin{pmatrix} 0 & -1 & 0 \\ 1 & 0 & -\sqrt{2} \\ 0 & \sqrt{2} & 0 \end{pmatrix} . \quad (5)$$

Δ is the anharmonicity also called qubit non-linearity. To drive the $0 \leftrightarrow 1$ transition without driving $1 \leftrightarrow 2$ the Ω_y quadrature has to be set to the derivative of $\Omega_x(t)$ scaled by $-1/2\Delta$. To show that few parameter pulses can be quickly calibrated, we assume that the anharmonicity is not known and that the initial pulse is a Gaussian with the wrong area

$$\Omega_{x,\text{initial}}(t) = A \exp\left\{-\frac{t^2}{2\sigma^2}\right\} \quad \Omega_{y,\text{initial}}(t) = 0.$$

Here A and σ are chosen at random. The calibration protocol has to find the correct values for A, σ and Δ such that the time evolution is

$$\hat{U}_{\text{target}} = \begin{pmatrix} 0 & 1 & 0 \\ 1 & 0 & 0 \\ 0 & 0 & e^{i\varphi} \end{pmatrix}$$

An example of the pulses are shown in Fig. 8. Figures 8(a) and 8(c) respectively show the pulses before and after the optimization which took only 76 evaluations of the fidelity function $\Phi = |\text{Tr}\{\hat{X}^\dagger \hat{U}\}|^2/9$. As can be seen by Fig. 8(b) the initial pulse is unable to drive any transitions since the amplitude of the pulse is too weak. The fidelity as function of iteration number for these pulses is shown in Fig. 9. Closed-loop optimization quickly finds the optimal pulse.

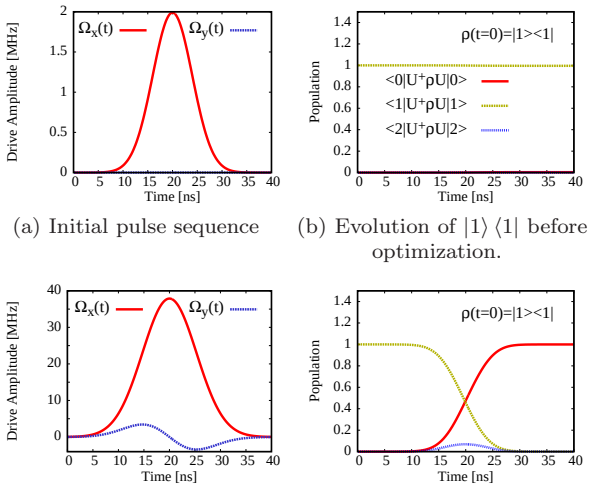

(a) Initial pulse sequence

(b) Evolution of $|1\rangle\langle 1|$ before optimization.

(c) Final pulse sequence

(d) Evolution of $|1\rangle\langle 1|$ after optimization.

FIG. 8. (color online) Control pulse of a weakly non-linear three level system. The target time evolution is an $\hat{X}$ gate. A bad initial pulse fails to produce the desired time evolution. (a) and (b) show the initial pulse and the corresponding population evolution when starting with $|1\rangle\langle 1|$. The final pulse, found after few iterations, produces an $\hat{X}$ gate while minimizing leakage, see (c) and (d) respectively for pulse and population as function of time.

Application of Ad-HOC to the Qubit-Bus-Qubit Architecture

Using the rotating wave approximation, the Hamiltonian of the qubit-bus-qubit architecture in the frame rotating at the frequency of the bus is

$$\hat{H} = \sum_{i=1}^{2} \delta_i(t)\hat{\sigma}_i^+\hat{\sigma}_i^- + \Delta_i |2\rangle_{ii}\langle 2| + \frac{g_i}{2}\left(\hat{\sigma}_i^+\hat{a} + \hat{\sigma}_i^-\hat{a}^\dagger\right)$$
$$= \hat{H}_\text{d} + \sum_{i=1}^{2} \delta_i(t)\hat{H}_{\text{c},i} \,. \quad (6)$$

The qubits are modeled as anharmonic three level systems with creation operators $\hat{\sigma}_i^+$ and non-linearity Δ_i. They are coupled to the bus with strength g_i. The bus creation operator is $\hat{a}^\dagger$. The parameters g_i and Δ_i need to be measured resulting in parameter errors. We approximate the control transfer chain by convoluting the

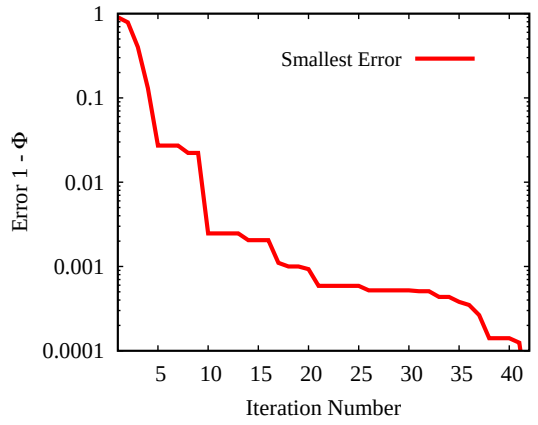

FIG. 9. Improvement of the fidelity as function of iteration number for the pulses of Fig. 8.

pulse with a Gaussian function of standard deviation σ_{filt}. The open loop optimization is done by gradient search with the quasi-Newton method BFGS [25]. In experiments the effect of the electronics is not as simple but can be taken into account by deconvoluting the controls with a measured transfer function. Imprecisions in this measurement further introduce errors. We model this by promoting the standard deviation of our Gaussian convolution function to a random variable following a Gaussian distribution. Lastly calibration errors between the output of the AWG and the qubit frequency can cause the qubit to over or under estimate the qubit-bus resonance point [18]. Since it is this resonance point which is most crucial to the gate we model it by a DC offset of $\Delta\omega_{\text{b},i}$ on the controls. This introduces the error term

$$\hat{H}_{\text{err}} = \sum_{i=1}^{2} \Delta\omega_{\text{b},i}\hat{\sigma}_i^+\hat{\sigma}_i^-$$

in the Hamiltonian (6), it now reads $\hat{H}' = \hat{H} + \hat{H}_{\text{err}}$. This error term is difficult to control since $[\hat{H}_{\text{c},i}, \hat{H}_{\text{err}}] = 0$. Furthermore, in practice $\Delta\omega_{\text{b},i}$ is not perfectly known and is therefore promoted to a random variable. In summary the parameters used in the model are given in Tab. I.

Optimization with Gate-Taylored Quality Parameters

The main text emphasizes randomized benchmarking as the fidelity measure. This fidelity is applicable when the desired gate is a Clifford gate. Here is shown that a gate specific fidelity can also be used to calibrate the pulse. We illustrate this with the optimization of a CZ gate. We define the following fidelity measure

$$\Phi_{\text{cz}} = \sum_{ij\in\{01,10,11\}} \frac{|U_{ij,ij}|^2}{6}\left[1 + (-1)^{ij}\cos\left(\arg\left(U_{ij,ij}\right)\right)\right].$$

Here $U_{ij,ij}$ is the element of the time evolution operator mapping the state $|ij\rangle$ onto itself. The terms $|U_{ij,ij}|^2$ are the qubit populations after the pulse sequence for a specific input state. The argument of these terms can be found using Ramesy measurements. A gate that is unitary and optimizes Φ_{cz} has to be a good CZ gate. An example of this fidelity as function of the iteration number is shown in Fig. 10. The initial pulse was optimized by GRAPE up to 80% fidelity using $\Phi = |\text{Tr}\{\hat{U}_{\text{cz}}^\dagger\hat{U}\}|^2/d^2$. The remaining calibration was done with the model free part of Ad-HOC. The target fidelity was set to be $\Phi_{\text{cz}} = 99.9\%$. It can be seen that the intrinsic gate fidelity follows closely.

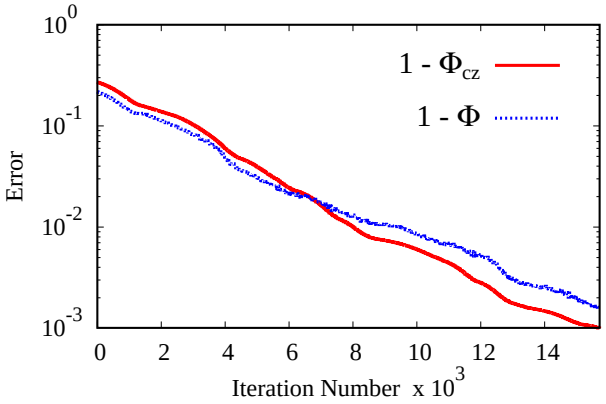

FIG. 10. (color online) Model free calibration with a gate tailored fidelity. At each iteration the gate overlap fidelity is also computed and, as can be seen, optimizing Φ_{cz} also optimizes Φ.

Noise Threshold

Fig. 6 of the main text shows that the closed-loop optimization stops when it can no longer tell, on average, if the changes in fidelity are due to noise or changes in the pulse parameters. The noisy fidelity used was

$$\Phi_{\text{noisy}} = \frac{n}{md} + \frac{m-n}{m}\Phi$$

where n is the number of times the channel depolarized out of a total of m trials. d is the Hilbert space dimension. Therefore the uniform probability of depolarization p is estimated by n/m. In order for the closed loop part of Ad-HOC to converge it must be able to distinguish if a new pulse sequence is better or worse. This sets bounds on the amount of noise tolerated. Thus when, on average, an operation on the simplex improves Φ of the worst pulse by less than a threshold difference $\Delta\Phi_{\text{th.}}$ the optimization will not be able to improve the fidelity any longer because the experiment cannot distinguish fidelities sufficiently

TABLE I. Parameters used in the model. The coupling strength g is given as function of the Qubit-Bus swap time by $(2T_{\mathrm{swap}})^{-1}$. The imprecision is given relative to the parameter it refers to. When promoting the parameters to random variables this imprecision serves as standard deviation. When performing the closed loop optimization, the AWG voltage calibration $\Delta\omega_{\mathrm{b},i}$ is chosen randomly with mean zero and standard deviation of 0.1% of the bus frequency. System realizations with unphysical parameters are discarded, e.g. σ_{filt} cannot be smaller than zero.

Name	Symbol	Qubit 1	Qubit 2	unit	Imprecision
Qubit-Bus Swap Time	$T_{\mathrm{swap},i}$	12.6	9.2	ns	-
Qubit-Bus Coupling Strength	g_i	40	54	MHz	4.0%
Qubit non-linearity	Δ_i	-59	-71	MHz	4.0%
Bus Frequency	ω_{b}	6.1		GHz	0.1%
Convolution function error	σ_{filt}	1		ns	40.0%

well. For this case, the threshold difference is

$$\Delta\Phi_{\mathrm{th.}} = \frac{d\Phi_{\mathrm{dep.}} - \bar{p} - \sigma_p}{d(1-\bar{p}-\sigma_p)} - \frac{d\Phi_{\mathrm{dep.}} - \bar{p} + \sigma_p}{d(1-\bar{p}+\sigma_p)}\,.$$

The estimation of p is $\bar{p} \pm \sigma_p = n/m \pm 1/12\sqrt{m}$. Here the factor 12 comes from the uniform distribution.

[1] M. A. Nielsen and I. L. Chuang, *Quantum Computing and Quantum Information* (Cambridge University Press, 2000).

[2] A. N. Boto, P. Kok, D. S. Abrams, S. L. Braunstein, C. P. Williams, and J. P. Dowling, Phys. Rev. Lett. **85**, 2733 (2000).

[3] S. Rice and M. Zhao, *Optical Conrol of Molecular Dynamics* (Wiley, 2000).

[4] P. Brumer and M. Shapiro, *Principles of the Quantum Control of Molecular Processes* (Wiley, 2003).

[5] A. Spörl, T. Schulte-Herbrueggen, S. Glaser, V. Bergholm, M. Storcz, J. Ferber, and F. Wilhelm, Phys. Rev. A **75**, 012302 (2007).

[6] N. Khaneja, T. Reiss, C. Kehlet, T. Schulte-Herbrüggen, and S. J. Glaser, J. Magn. Reson. **172**, 296 (2005).

[7] S. Glaser, T. Schulte-Herbrüggen, M. Sieveking, O. Schedletzky, N. Nielsen, O. Sorensen, and C. Griesinger, Science **280**, 421 (1998).

[8] T. Boreneman, M. Hurliman, and D. Cory, J. Magn. Res. **207**, 220 (2010).

[9] M. Lapert, G. Ferrini, and D. Sugny, Phys. Rev. A **85**, 023611 (2012).

[10] R. Schmidt, A. Negretti, J. Ankerhold, T. Calarco, and J. T. Stockburger, Phys. Rev. Lett. **107**, 130404 (2011).

[11] P. Doria, T. Calarco, and S. Montangero, Phys. Rev. Lett. **106**, 190501 (2011).

[12] A. Castro, J. Werschnik, and E. Gross, Phys. Rev. Lett. **109**, 153603 (2012).

[13] R. Bücker, J. Grond, S. Manz, T. Berrada, T. Betz, C. Koller, U. Hohenester, T. Schumm, A. Perrin, and J. Schmiedmayer, Nat. Phys. **7**, 608 (2011).

[14] G. Jäger and U. Hohenester, Phys. Rev. A **88**, 035601 (2013).

[15] R. Nigmatullin and S. G. Schirmer, New Journal of Physics **11**, 105032 (2009).

[16] S. Montangero, T. Calarco, and R. Fazio, Phys. Rev. Lett. **99**, 170501 (2007).

[17] F. Motzoi, J. M. Gambetta, P. Rebentrost, and F. K. Wilhelm, Phys. Rev. Lett. **103**, 110509 (2009).

[18] D. Egger and F. K. Wilhelm, Superconductor Science and Technology **27**, 014001 (2014).

[19] M. Hellgren, E. Räsänen, and E. K. U. Gross, Phys. Rev. A **88**, 013414 (2013).

[20] R. S. Judson and H. Rabitz, Phys. Rev. Lett. **68**, 1500 (1992).

[21] J. Clarke and F. K. Wilhelm, Nature **453**, 1031 (2008).

[22] F. Motzoi, J. M. Gambetta, S. T. Merkel, and F. K. Wilhelm, Phys. Rev. A **84**, 022307 (2011).

[23] P. Owrutsky and N. Khaneja, Phys. Rev. A **86**, 022315 (2012).

[24] B. Khani, S. T. Merkel, F. Motzoi, J. M. Gambetta, and F. K. Wilhelm, Phys. Rev. A **85**, 022306 (2012).

[25] F. F. Floether, P. de Fouquieres, and S. G. Schirmer, New Journal of Physics **14**, 073023 (2012).

[26] J. A. Nelder and R. Mead, Comput. J. **7**, 308 (1967).

[27] E. Magesan, J. M. Gambetta, B. R. Johnson, C. A. Ryan, J. M. Chow, S. T. Merkel, M. P. da Silva, G. A. Keefe, M. B. Rothwell, T. A. Ohki, M. B. Ketchen, and M. Steffen, Phys. Rev. Lett. **109**, 080505 (2012).

[28] J. M. Chow, J. M. Gambetta, L. Tornberg, J. Koch, L. S. Bishop, A. A. Houck, B. R. Johnson, L. Frunzio, S. M. Girvin, and R. J. Schoelkopf, Phys. Rev. Lett. **102**, 090502 (2009).

[29] E. Magesan, J. M. Gambetta, and J. Emerson, Phys. Rev. Lett. **106**, 180504 (2011).

[30] J. Kelly and R. Barends, "Optimal quantum control using randomized benchmarking," In preparation.

[31] M. Mariantoni, H. Wang, T. Yamamoto, M. Neeley, R. C. Bialczak, Y. Chen, M. Lenander, E. Lucero, A. D. O'Connell, D. Sank, M. Weides, J. Wenner, Y. Yin, J. Zhao, A. N. Korotkov, A. N. Cleland, and J. M. Martinis, Science **334**, 61 (2011).

[32] A. G. Fowler, M. Mariantoni, J. M. Martinis, and A. N. Cleland, Phys. Rev. A **86**, 032324 (2012).

[33] A. Galiautdinov, A. N. Korotkov, and J. M. Martinis, Phys. Rev. A **85**, 042321 (2012).

[34] E. Lucero, R. Barends, Y. Chen, J. Kelly, M. Mariantoni, A. Megrant, P. O'Malley, D. Sank, A. Vainsencher, J.Wenner, Y. Y. T. White, A. N. Cleland, and J. M. Martinis, Nature Physics **8**, 719 (2012).

[35] M. J. Biercuk, H. Uys, A. P. VanDevender, N. Shiga, W. M. Itano, and J. J. Bollinger, Nature **458**, 996 (2009).

[36] R. Barends, J. Kelly, A. Megrant, A. Veitia, D. Sank, E. Jeffrey, T. C. White, J. Mutus, A. G. Fowler, B. Campbell, Y. Chen, Z. Chen, B. Chiaro, A. Dunsworth, C. Neill, P. O'Malley, P. Roushan, A. Vainsencher, J. Wenner, A. N. Korotkov, A. N. Cleland, and J. M. Martinis, "Logic gates at the surface code threshold: Superconducting qubits poised for fault-tolerant quantum computing," ArXiv:1402.4848.

[37] T. E. Skinner, T. O. Reiss, B. Luy, N. Khaneja, and S. J. Glaser, J. Magn. Res. **163**, 8 (2003).

[38] J. M. Gambetta, F. Motzoi, S. T. Merkel, , and F. K. Wilhelm, Physical Review A **83**, 012308 (2011).